

# 2,4-Toluene Diisocyanate Detection in Liquid and Gas Environments Through Electrochemical Oxidation in an Ionic Liquid

Lu Lin, Abdul Rehman, Xiaowei Chi, Xiangqun Zeng\*

Department of Chemistry, Oakland University, Rochester, MI 48309, USA

\* Corresponding Author (Email: [zeng@oakland.edu](mailto:zeng@oakland.edu))

## Supplementary Information

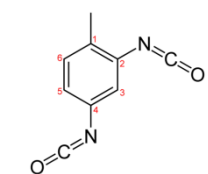
**Table S1. Summary of the current techniques for the sensing of TDI and its derivatives.**

Technique	Subject of Study	Sampling Process	Limit of Detection	Limitation	Ref.
HPLC	all TDI compounds	samples separated with column	2 ppb at sampled air volume of 20 L	expensive instrumentation, longer sampling time reduces the accuracy	9
CGC	mixtures of isocyanates and amines in air	converts isocyanate group into urethane, then extract to amide	in the order of 40-80 fmol	expensive instrumentation, requires derivatization and extraction steps	10
GC-MS	toluenediamine (TDA) in hydrolysed human urine and blood plasma	converts TDA to the perfluoro-fatty acid anhydride derivatives	0.05 $\mu$ l of TDA in human urine or plasma	expensive instrumentation, requires derivatization and extraction steps	11
IC	TDIs in synthetic rubber track	hydrolyze TDI to TDA, then separate the sample.	0.13 mg/L	expensive instrumentation, requires derivatization and extraction steps	13
IR	NCO groups	absorption band at 2275~2230 $\text{cm}^{-1}$	8 $\mu\text{g/ml}$	expensive instrumentation, found to be inadequately sensitive	16
Colorimetry	unreacted isocyanates in urethane-based polymers	unreacted amine determined colorimetrically with molachite green	0.5%	has interference problems especially from humidity in the air	15
ELISA	aromatic diisocyanates (dNCO) adducts	utilizing aromatic dNCO-specific monoclonal antibodies (mAbs) for the detection	<0.10 ng/mL in adducts; 7.64 ng/mL in human serum	lacks the specificity	17
Piezoelectric Crystal Detector	2,4-TDI in air	coats the crystals by silicone material	10 ppb	unsuitable in humid environments	18
IL-based Amperometric Sensor	2,4-TDI in air and in IL [C <sub>4</sub> mpy][NTf <sub>2</sub> ]	direct transduction signal readout	0.786 ppm in air; 130 ppm in IL	This is a destructive examination	This work

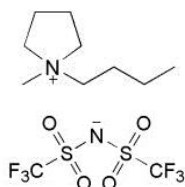
Note: HPLC – High Performance Liquid Chromatography, CGC – Capillary Gas Chromatography, GC-MS – Gas Chromatography Mass Spectrometry, IC – Ion Chromatography, IR – Infrared Spectroscopy, ELISA – Enzyme Linked Immunosorbent Assays.

There're two major types of detection techniques for isocyanates and their amine and amide derivatives due to the significant needs in monitoring them in environment. One uses the expensive instruments such as HPLC, CGC, GC-MS, IC and IR that commonly exhibit low limit of detection and excellent selectivity. But they are bench top instruments and also require complicated and time-consuming sampling processes for the detection. Another type including colorimetry, ELISA, and piezoelectric crystal detector uses low cost and simple instrumentations that have potential for miniaturization. But they suffer limitations for real world application especially at high level of humidity. In general, they also encounter the problem of poor selectivity.

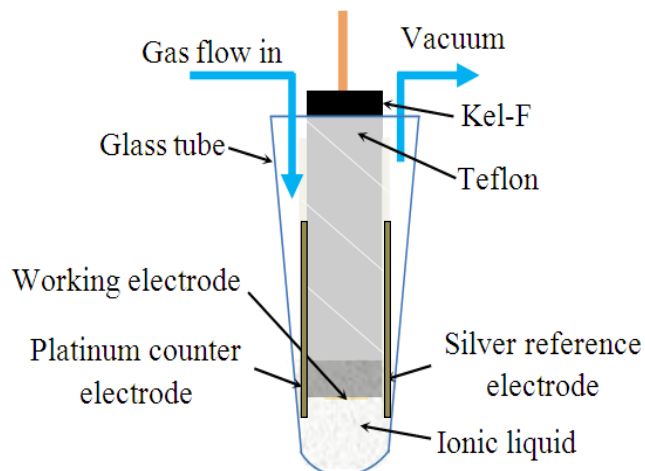
Our proposed IL-based amperometric sensor takes the advantages of the characteristics of electrochemical sensor. The uses of low cost carbon electrode material and non-volatile IL electrolyte make it a promising low cost and miniaturized disposal sensor. The electrochemical detection based on the oxidation of isocyanate functional group provides good selectivity and there is very little water present in the hydrophobic IL used in this study, thus, very little isocyanates can be lost due to the chemical reactions that occur at conventional solvents such as water, alcohol, acids and organic solvents that contain primary and secondary amine. This benefit makes it much more powerful and lower cost detection technology.



**(A) 2,4-TDI**

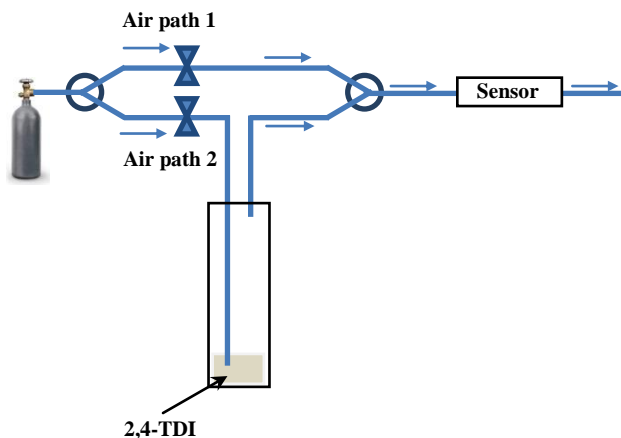


**(B) [C<sub>4</sub>mpy][NTf<sub>2</sub>]**



**(C) Schematic of the Electrochemical Cell**

Scheme S1. Chemical structures of (A) the analyte 2,4-toluene diisocyanate, (B) the ionic liquid 1-butyl-1-methylpyrrolidinium bis(trifluoromethylsulfonyl) imide, and (C) schematic of the Electrochemical cell in a flow system. Glassy carbon and gold are used as working electrode materials in different experiments. The reference electrode and counter electrode are silver and platinum wires, respectively.



Scheme S2. Cross-section of the sampling system for real-time gas phase 2,4-TDI detection via chronoamperometry. Two gas paths were designed to adjust the amount of gas phase 2,4-TDI that was purged into the sensor. Total gas flowrate was 200 scm.

## The Calculations of TDI Concentration

The cross-section of the gas sampling is presented in Scheme S2. We have a three-way valve connected to the outlet of the air gas cylinder. There are two air paths, of which path 2 goes into the TDI sample reservoir and bubbles out the gas phase TDI sample, and mixes with the air in the path 1. The TDI gas concentration can therefore be controlled when adjusting the flows in path 1 and 2. The volume of TDI gas in path 2 can be calculated according to Dalton's Law of Partial Pressures ( $V_{TDI} = \frac{P_{TDI} \times V_{path2}}{P_{path2}}$ ), and the concentration of this TDI analyte can thus be obtained. TDI has a vapor pressure of 0.05 mm Hg, which equals to 6.666 Pa. For example, if the flows are 180 sccm and 20 sccm for path 1 and 2, respectively. Then,  $V_{TDI} = 6.67 \text{ (Pa)} * 20 \text{ (sccm)} / 101325 \text{ (Pa)} = 0.001316 \text{ (sccm)}$ . Thus, concentration of TDI in ppm will be  $0.001316 \text{ (sccm)} / 200 \text{ (sccm)} = 6.58$ .

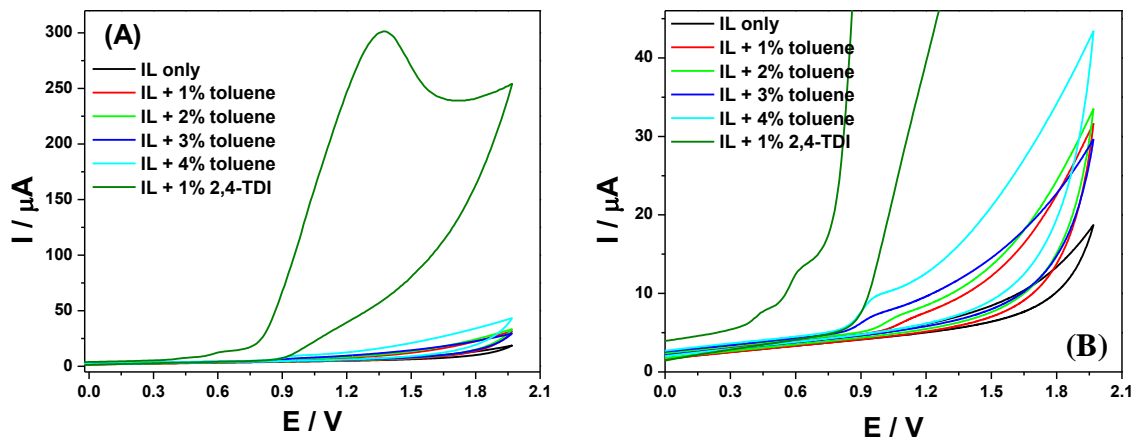


**Figure S1.** (A) CV of [C<sub>4</sub>mpy][NTf<sub>2</sub>] adding different amount of toluene sample and 1% of 2,4-TDI sample. Glassy carbon, silver and platinum electrodes were used as the working, reference and counter electrodes, respectively. Scan rate was 100 mV/s. All potentials were calibrated based on the Fc/Fc<sup>+</sup> redox couple. Air was used as background gas. (B) The enlarged view of the oxidation peak of toluene in [C<sub>4</sub>mpy][NTf<sub>2</sub>].

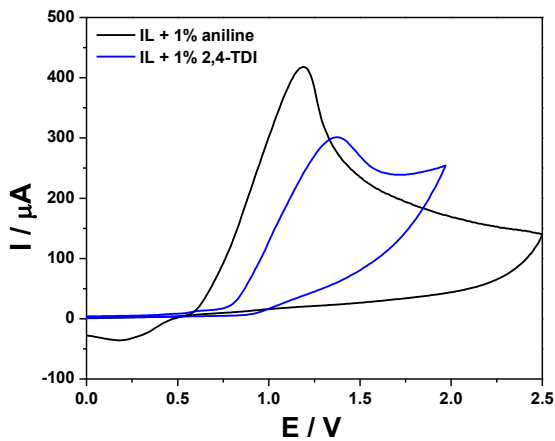


**Figure S2.** CV of [C<sub>4</sub>mpy][NTf<sub>2</sub>] adding 1% aniline and 1% 2,4-TDI, showing similar peak currents and different peak potentials. Glassy carbon, silver and platinum electrodes were used as the working, reference and counter electrodes, respectively. Scan rate was 100 mV/s. All potentials were calibrated based on the Fc/Fc<sup>+</sup> redox couple. Air was used as background gas.

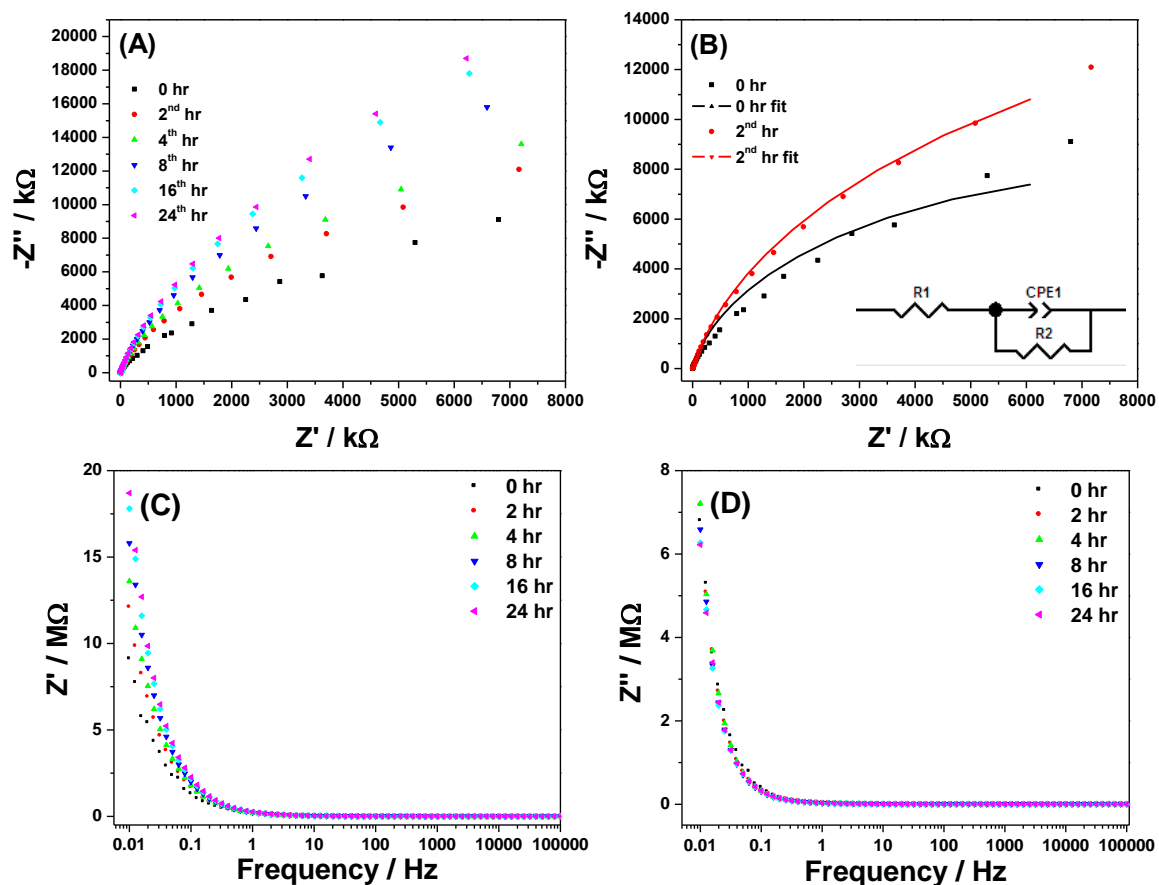


Figure S3. (A) Nyquist plot measured at various time intervals with 1% v/v 2,4-TDI in  $[C_4mpy][NTf_2]$  on glassy carbon electrode, in air condition. Silver wire and platinum wire were the reference and counter electrodes, respectively. AC bias was 5 mV, and the DC input was 0 V vs. open circuit. (B) Fitting of impedance spectra measured at 0 hr and 2<sup>nd</sup> hr. The solid lines are the results of fitting to the equivalent circuit presented in the insert. (C) The Bode plots of  $Z'$  (the real part of the impedance) changes at different frequencies. (D) The Bode plots of  $Z''$  (the imaginary part of the impedance) changes at different frequencies. The EIS experimental parameters: AC bias was 5 mV, and the DC input was 0 V vs. open circuit. Air is the background gas.

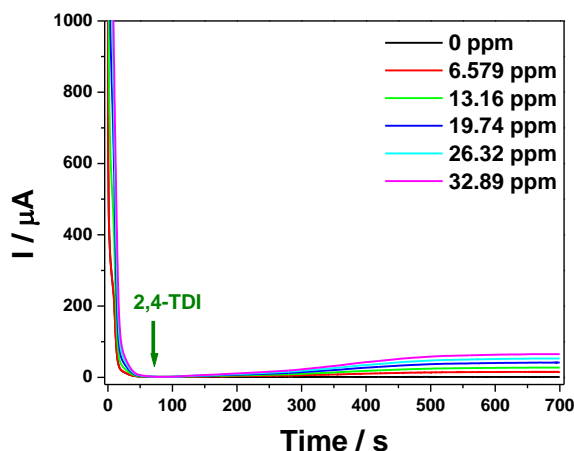


Figure S4. Real time chronoamperometry detection of gas phase 2,4-TDI in  $[C_4mpy][NTf_2]$ . External potential was set constant at 1.4 V. Air was the background gas. Data sampling rate is 0.2 second per data point. 2,4-TDI flow was added at the 70<sup>th</sup> second.

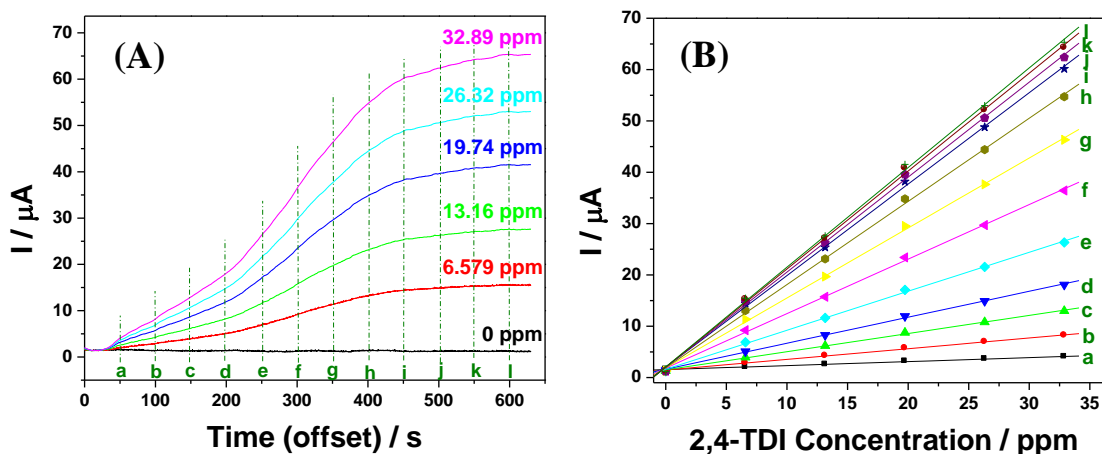


Figure S5. (A) Chronoamperometry data in Figure S3 with time offset. Vertical olive dash dot lines mark the time scales for sensing signal calibration. External potential was 1.4 V, calibrated based on ferrocene (II/III) redox couple. Air was the background gas. Data sampling rate is 0.2 second per data point. (B) The corresponding calibration curves: a)  $y=0.07762x+1.556$ ,  $R^2=0.9967$ ; b)  $y=0.2083x+1.460$ ,  $R^2=0.9985$ ; c)  $y=0.3540x+1.500$ ,  $R^2=0.9985$ ; d)  $y=0.5063x+1.627$ ,  $R^2=0.9989$ ; e)  $y=0.7598x+1.617$ ,  $R^2=0.9988$ ; f)  $y=1.063x+1.829$ ,  $R^2=0.9989$ ; g)  $y=1.363x+1.875$ ,  $R^2=0.9990$ ; h)  $y=1.621x+1.901$ ,  $R^2=0.9991$ ; i)  $y=1.782x+2.054$ ,  $R^2=0.9990$ ; j)  $y=1.851x+2.030$ ,  $R^2=0.9991$ ; k)  $y=1.909x+2.051$ ,  $R^2=0.9990$ ; l)  $y=1.942x+2.076$ ,  $R^2=0.9990$ .

**Table S2. Detail values of sensitivity, LOD and T90 at various sensor function time.**

<b>Sensor Function Time (s)</b>	<b>Sensitivity (<math>\mu\text{A/ppm}</math>)</b>	<b>LOD (ppm)</b>	<b>T90 (s)</b>
50	0.07762	41.48	48.96
100	0.2083	12.46	90.80
150	0.3540	6.822	138.3
200	0.5063	5.064	185.8
250	0.7598	2.709	237.5
300	1.063	2.030	288.3
350	1.363	1.420	325.4
400	1.621	1.107	366.0
450	1.782	0.9703	398.4
500	1.851	0.8887	409.6
550	1.909	0.8177	423.4
600	1.942	0.7693	432.3